Topic No. 1.11 Modeling, Numerical Simulation (and AI) Abstract Reference No: 0089
Topic No. 9.04 Fuel Cells and Electrolyzers
Oral or Poster

COMPUTATIONAL FACILITATION OF LARGE SCALE MICROFLUIDIC FUEL CELL ARCHITECTURES – POWERING THE FUTURE

Michel Takken[1] and Robert Wille[1,2,3]
[1]Technical University Munich, GERMANY
[2]Software Competence Center Hagenberg GmbH, AUSTRIA
[3]Munich Quantum Software Company GmbH, GERMANY

We propose a rapid simulation method which facilitates the development of large scale microfluidic fuel cell architectures. Microfluidic fuel cells provide great control of flow and thermal management, which are otherwise challenging tasks in conventional fuel cells. However, to match the power performance of their macrofluidic counterparts, large scale architectures would be required. We propose a rapid simulation method that, for the first time, can accurately simulate architectures with 16,000 cells within an hour on a single CPU core, facilitating the development of large scale microfluidic fuel cell architectures, which can be used to power, e.g., a mid-size drone.

Microfluidic fuel cells have been actively developed and successfully been stacked into fuel cell stacks, similar to conventional fuel cells [1]. Simultaneously, the fabrication of microfluidic devices with integrated electrodes and (rapid) 3D printing techniques enable us to produce devices with large scale microfluidic fuel cell architectures in reasonable time [2]. To facilitate the development of such large scale, and likely complex, architectures computational methods, such as simulation, are essential. However, state-of-the-art simulation methods, such as *Computational Fluid Dynamics* (CFD), scale poorly and, hence, cannot be used for this purpose.

The proposed method employs an abstract simulation method that simulates the concentration of species throughout a microfluidic network [3] and couples these concentrations with the Nernst and Butler-Volmer equations to obtain the polarization curve of a single cell (see Fig. 1). At the electrodes, the propagation of concentration is modeled using the Sturm-Liouville theorem to account for the reaction rate and, hence, the boundary conditions that follow from the local electrochemical reactions. This concept is extended for a fuel cell architecture, which is formed by a flow network and an electrical network that intersect at the set of fuel cells in the architecture, as illustrated in Fig. 2. This results in a non-linear system of equations, which provides the total voltage for an operating current, eventually leading to the architecture's polarization curve.

The proposed method was implemented in C++ and the resulting polarization and power density curves for a single cell were compared to those obtained from CFD simulations conducted with COMSOL Multiphysics®. These curves are provided in Fig. 3. Moreover, the hydrogen concentration fields, as obtained by the proposed method and the CFD software, showed a strong agreement and are illustrated in Fig. 4. Concentration fields of other species showed similar agreement. Furthermore, the method's performance was assessed, based on runtimes for various problem sizes n and architectures. The obtained runtimes are listed in Table I. As a reference, the simulation for a single cell using the CFD software took 63 seconds. From this it can be concluded that the method is accurate and scales well. Keeping in mind that the runtimes can be further improved with parallel implementation and that multiple devices with an architecture can be combined into stacks, it is now possible to consider microfluidic fuel cell systems to power macroscale devices, such as a mid-size drone.

REFERENCES

1. Wang, Yifei, et al. "Microfluidic fuel cells with different types of fuels: A prospective review." *Renewable and sustainable energy reviews* 141 (2021): 110806.
2. Selemani, Major A., et al. "3D printed microfluidic devices with electrodes for electrochemical analysis." *Analytical Methods* (2024).
3. Takken, Michel, Maria Emmerich, and Robert Wille. "An Abstract Simulator for Species Concentrations in Channel-Based Microfluidic Devices." *IEEE Transactions on Computer-Aided Design of Integrated Circuits and Systems* (2025).

DOI 10.70477/UKFG9855

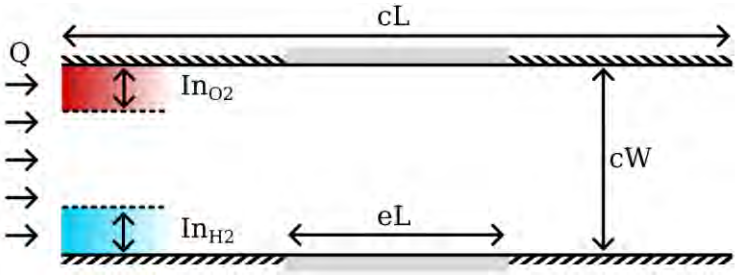

Fig. 1: A fuel cell channel with length cL and width cW, and an anode and cathode of length eL on the bottom and top, respectively. The electrolyte enters the channel on the left, with flow rate Q. The lower and upper bands of the inflowing electrolyte contain concentrated hydrogen and oxygen, respectively.

Fig. 2: A schematic representation of a device with an architecture composed of a flow network and an electrical network. The flow network can be represented as a *Directed Acyclic Graph* (DAG), with in- and outlets. The electrical network can be represented as a *Tree,* with parallel or series connections between nodes. The grey nodes are microfluidic fuel cells.

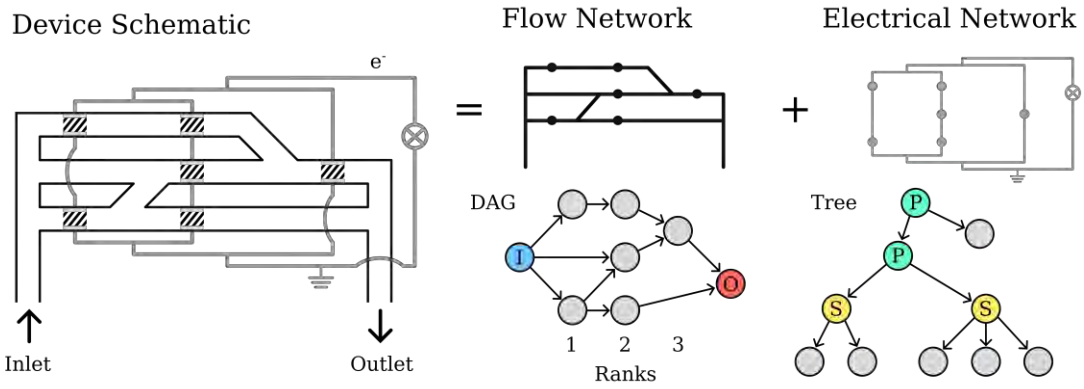

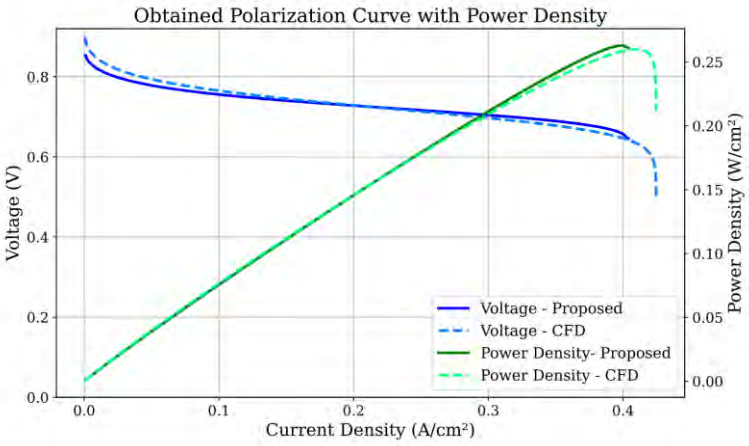

Fig. 3: The polarization curve (Voltage) and the corresponding power density curve as obtained with the proposed method and the CFD software, COMSOL Multiphysics®.

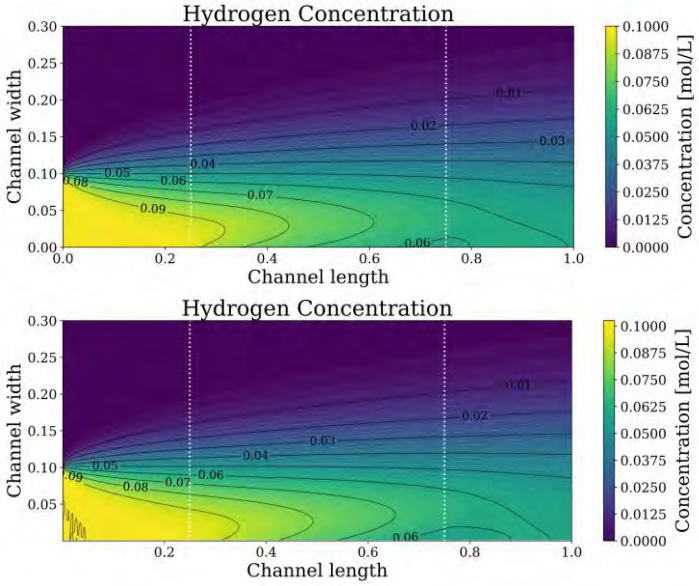

Fig. 4: The hydrogen concentration field, at an operating current density of 0.1 A/cm^2, as obtained with the proposed method (top) and the CFD software, COMSOL Multiphysics® (bottom).

Table I: The obtained runtimes of the proposed method for architectures with increasing number of fuel cells (n). Nine different architectures were considered with different r_{DAG} and r_{Tree} values. Here, r_{DAG} describes whether the flow network is fully in parallel (0.0), or series (1.0), or has a quasi-square shape ($\sqrt{n}$). Similarly, r_{Tree} gives the ratio of connections that are in series.

Runtimes [mm:ss.ss]

	$r_{DAG} = 0.0$			$r_{DAG} = \sqrt{n}$			$r_{DAG} = 1.0$		
n	$r_{Tree} = 0.0$	$r_{Tree} = 0.5$	$r_{Tree} = 1.0$	$r_{Tree} = 0.0$	$r_{Tree} = 0.5$	$r_{Tree} = 1.0$	$r_{Tree} = 0.0$	$r_{Tree} = 0.5$	$r_{Tree} = 1.0$
64	00:04.23	00:04.11	00:04.21	00:04.28	00:04.21	00:04.46	00:04.51	00:04.54	00:04.39
256	00:16.91	00:16.35	00:16.55	00:18.18	00:17.88	00:17.95	00:17.91	00:18.19	00:17.17
1024	01:07.66	01:05.40	01:09.16	01:11.02	01:11.04	01:09.75	01:12.63	01:09.10	01:13.04
4096	04:52.83	05:26.89	05:16.85	05:38.12	05:00.82	04:54.13	05:38.47	05:30.44	05:40.82
16384	19:28.53	21:23.83	22:12.37	22:49.83	21:32.20	23:43.20	22:54.74	23:09.82	22:37.10